

A NEW SHORT-PERIOD BLUE VARIABLE*

ARLO U. LANDOLT

Louisiana State University Observatory and Kitt Peak National Observatory†

Received October 27, 1967; revised December 14, 1967

ABSTRACT

Photoelectric data which point to a 12^m.5 variation in the brightness of a white-dwarf-like star are discussed.

A star previously reported in the literature (Haro and Luyten 1961) as a candidate for membership in the white-dwarf classification of stellar objects has been found to be variable in light. The object, projected against a dark cloud in Taurus, has the 1965 position as recorded at the telescope console of $\alpha = 4^{\text{h}}16^{\text{m}}50^{\text{s}}$, $\delta = +27^{\circ}13'24''$; therefore, $l^{\text{II}} = 169^{\circ}.8$ and $b^{\text{II}} = -16^{\circ}.0$. A finding chart for the blue variable, together with the comparison stars used in the photometric study to be described below, is given in Figure 1 (Plate 4).

Photoelectric observations have been made on the *UBV* system on two nights at the No. 1 36-inch and on three nights at the 84-inch reflecting telescopes of the Kitt Peak National Observatory. Some of the three-color observations of this star were obtained on December 5 and 11, 1964, U.T., nights primarily devoted to another, larger photometric program. The observation and reduction techniques employed have been described elsewhere (Landolt 1967). Those data, collected through use of a refrigerated 1P21 photocell together with the standard *UBV* filters, yielded external probable errors of ± 0.018 mag in *V*, ± 0.014 mag in $(B - V)$, and ± 0.018 mag in $(U - B)$. The observing procedure at the telescope in December 1965 and 1966 was the same as in 1964 (Landolt 1967). However, since the brightness of the blue variable changed appreciably within a time interval measured in minutes, as will be shown in what follows, each set of *y*, *b*, *u* deflections was reduced to give a *V* magnitude and $(B - V)$ and $(U - B)$ color indices.

The majority of the photoelectric observations were made in December 1965 and 1966 under rather poor atmospheric conditions. Only the blue variable, its comparison stars, and a few standards were monitored. Since one could visually watch the blue variable change in brightness on the Brown recorder chart paper from one measurement to the next, the decision was made to return to the primary comparison star C1 every 20 minutes or so. However, even with a very generous allotment of telescope time, the weather just did not co-operate. This fact, together with the method of observation, did not make available as many intercomparisons of the comparison stars as one might like. Hence, possible small variations in an individual comparison star cannot be entirely ruled out. Their magnitudes and colors are listed in Table 1. The positions given were read from the telescope console.

The 393 three-color observations of the blue variable are given in Tables 2 and 3. The first column in each table gives the time of observation in heliocentric Julian days with an accuracy of ± 0.00005 day. On the discovery nights of December 5 and 11, 1964, U.T., time did not permit the selection of comparison stars. Therefore, the magnitudes and colors of the variable in Table 2 result from tie-ins to the *UBV* system standards

* *Contributions of the Louisiana State University Observatory*, No. 6; *Contributions of the Kitt Peak National Observatory*, No. 310.

† Operated by the Association of Universities for Research in Astronomy, Inc., under contract with the National Science Foundation.

PLATE 4

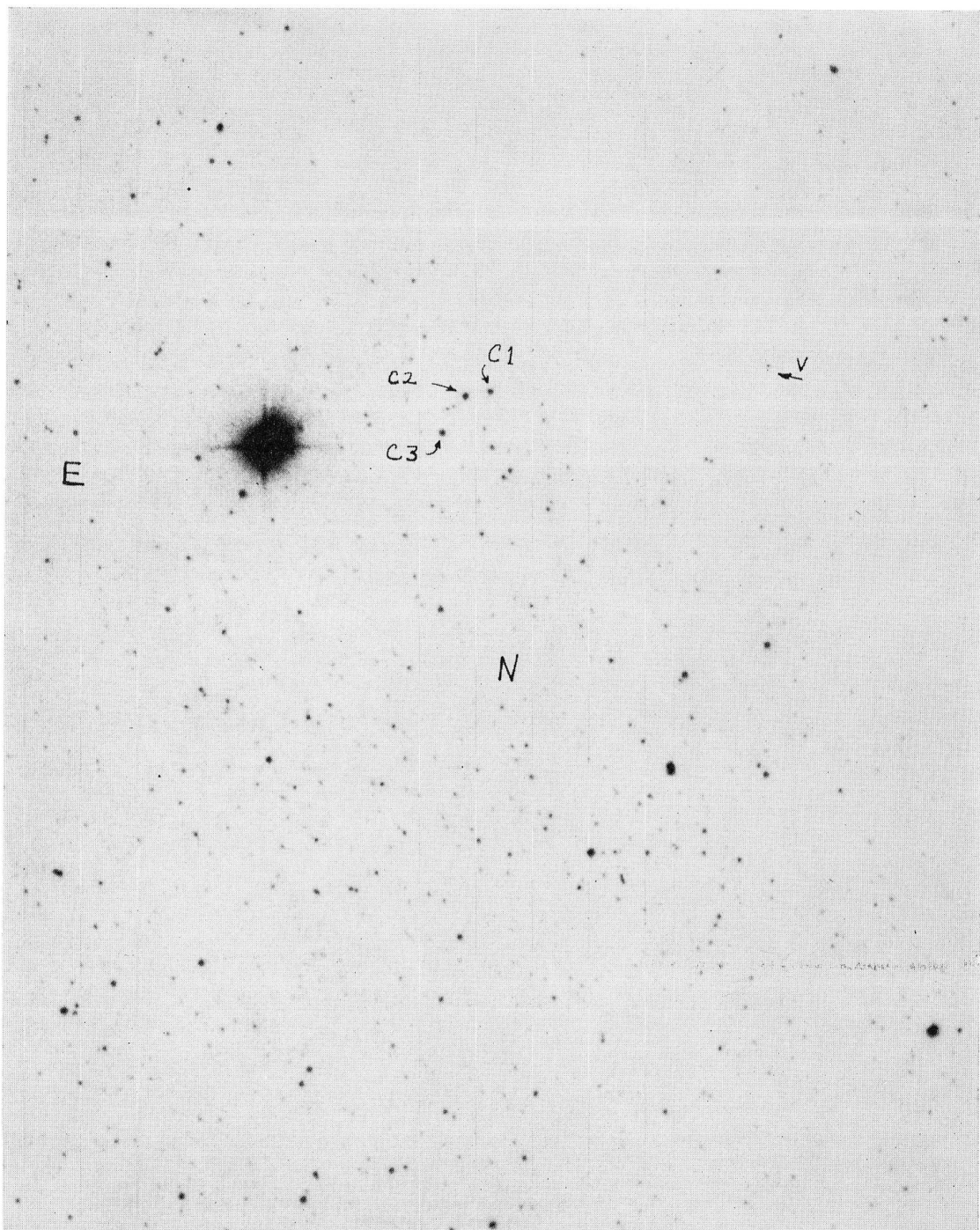


FIG. 1.—Finding chart for the blue variable made from *Palomar Sky Atlas* red print No. E 1454. The stars denoted C1, C2, and C3 were the comparison stars (see Table 1). The bright star is 52 Tauri = HR 1348 = HD 27382.

LANDOLT (*see* page 151)

which were being observed as part of another photometric program (Landolt 1967). The second, third, and fourth columns in Table 3 present ΔV , $\Delta(B - V)$, and $\Delta(U - B)$ through comparison of the primary standard C1 with the blue variable in the sense variable *minus* comparison star.

The light and color curves for the blue variable are shown in Figures 2-5. The gaps in the data plotted in these figures occur during time intervals when comparison-star and *UBV* standard-star observations were being made. The KPNO 84-inch observations of December 11, 1964, U.T. in Figure 2 actually first proved the blue star to be variable in brightness. To a greater or lesser degree, semiperiodic variations are apparent in Figures 3-5 also. Attempts to determine an accurate period of variation were made through use of a computer program (Kelsall 1966) designed to minimize the variance about a sine curve put through the data. Next, a periodogram analysis of the data was carried out via a computer program written by Hill (1967) based on techniques described by Wehlau and Leung (1964). Figure 6 shows a portion of the spectrum computed for December 26, 1965, U.T. from the raw data shown in Figure 4, in which a period interval between 5-60

TABLE 1
COMPARISON STARS

NAMES	1965 COORDINATES		V (mag)	B - V (mag)	U - B (mag)
	α	δ			
C1... ..	4 ^h 17 ^m 39 ^s	+27° 14' 17"	13.22	+1 18	+0 98
C2.....	14.69	+1 51	+1 24:
C3.....	4 17 41	+27 14 28	12.98	+2.00	+2.30

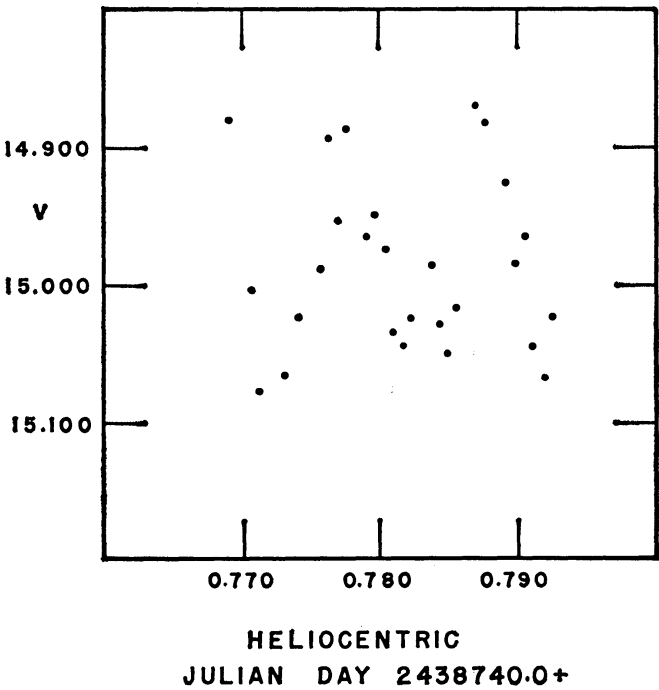


FIG. 2.—Plot of brightness variation in *V* versus heliocentric Julian day for the blue variable for December 11, 1964, U.T.

TABLE 2
UBV PHOTOELECTRIC MEASUREMENTS OF
THE BLUE VARIABLE

Heliocentric JD	<u>V</u>	<u>B-V</u>	<u>U-B</u>
2438734.8223	15.105	+0.143	-0.625
.8233	14.854	.194	-0.575
.8251	14.099	.323	-0.667
.8259	15.281	.136	-0.617
.8312	14.902	.336	-0.502
2438734.8322	14.826	.442	-0.647
2438740.7690	14.881	.131	-0.548
.7707	15.003	.142	-0.475
.7712	15.077	.121	-0.508
.7733	15.065	.159	-0.526
.7742	15.023	.244	-0.551
.7758	14.989	.229	-0.535
.7764	14.894	.340	-0.516
.7771	14.954	.103	-0.602
.7777	14.898	.084	-0.542
.7792	14.965	.144	-0.520
.7797	14.950	.192	-0.551
.7805	14.974	.213	-0.545
.7811	15.033	.152	-0.515
.7818	15.043	.187	-0.494
.7823	15.022	.221	-0.549
.7839	14.987	.274	-0.531
.7845	15.028	.223	-0.543
.7851	15.049	.201	-0.526
.7857	15.014	.286	-0.604
.7872	14.870	.167	-0.559
.7878	14.883	.211	-0.561
.7893	14.926	.276	-0.541
.7899	14.985	.201	-0.530
.7905	14.964	.206	-0.527
.7911	15.044	.173	-0.515
.7920	15.068	.189	-0.574
.7926	15.022	.267	-0.599

TABLE 3
DIFFERENTIAL *UBV* MAGNITUDES AND COLORS OF THE BLUE VARIABLE

Heliocentric JD	$\Delta \underline{V}$	$\Delta (\underline{B}-\underline{V})$	$\Delta (\underline{U}-\underline{B})$	Heliocentric JD	$\Delta \underline{V}$	$\Delta (\underline{B}-\underline{V})$	$\Delta (\underline{U}-\underline{B})$
2439000 114.6411	1.658	-1.027	-1.533	2439000. 114.6843	1.632	-0.978	-1.436
.6421	1.587	-0.943	-1.505	.6854	1.538	-0.836	-1.522
.6443	1.730	-0.905	-1.535	.6859	1.627	-0.904	-1.545
.6449	1.742	-0.885	-1.542	.6867	1.620	-0.934	-1.574
.6458	1.757	-0.892	-1.499	.6873	1.558	-0.927	-1.486
.6464	1.807	-0.950	-1.550	.6883	1.594	-0.868	-1.527
.6483	1.753	-0.915	-1.568	.6888	1.615	-0.848	-1.532
.6490	1.695	-0.952	-1.544	.6907	1.737	-0.951	-1.519
.6497	1.730	-1.069	-1.503	.6913	1.749	-0.927	-1.468
.6503	1.655	-0.891	-1.546	.6923	1.744	-0.887	-1.531
.6511	1.704	-0.887	-1.528	.6928	1.676	-0.928	-1.447
.6517	1.768	-1.052	-1.431	.6938	1.630	-0.928	-1.586
.6542	1.596	-0.910	-1.448	.6943	1.586	-0.954	-1.507
.6546	1.703	-0.985	-1.514	.6951	1.627	-0.967	-1.505
.6552	1.706	-0.921	-1.482	.6957	1.648	-0.975	-1.509
.6558	1.737	-0.914	-1.518	.6965	1.606	-0.873	-1.542
.6566	1.711	-0.918	-1.559	.6971	1.718	-0.996	-1.527
.6572	1.727	-0.933	-1.453	.6980	1.756	-1.010	-1.457
.6590	1.679	-0.924	-1.514	.6985	1.759	-0.966	-1.492
.6596	1.747	-0.991	-1.429	.7004	1.773	-1.003	-1.451
.6606	1.778	-1.019	-1.544	.7010	1.711	-0.924	-1.461
.6611	1.764	-0.958	-1.515	.7019	1.699	-0.949	-1.568
.6619	1.686	-0.907	-1.522	.7025	1.767	-1.001	-1.517
.6625	1.701	-0.885	-1.525	.7040	1.725	-0.967	-1.435
.6632	1.726	-0.906	-1.523	.7046	1.793	-1.001	-1.420
.6639	1.686	-0.900	-1.542	.7054	1.821	-0.955	-1.459
.6744	1.738	-0.894	-1.566	.7060	1.957	-1.101	-1.459
.6750	1.546	-0.732	-1.529	.7068	1.875	-0.967	-1.429
.6768	1.657	-0.846	-1.506	.7074	1.899	-1.016	-1.459
.6774	1.624	-0.846	-1.520	.7075	1.947	-1.008	-1.468
.6784	1.662	-0.814	-1.544	.7081	1.875	-1.042	-1.410
.6789	1.681	-0.873	-1.542	.7169	2.003	-0.896	-1.567
.6802	1.640	-0.844	-1.456	.7175	1.887	-0.865	-1.511

TABLE 3—Continued

Heliocentric JD	$\Delta \underline{V}$	$\Delta (\underline{B}-\underline{V})$	$\Delta (\underline{U}-\underline{B})$	Heliocentric JD	$\Delta \underline{V}$	$\Delta (\underline{B}-\underline{V})$	$\Delta (\underline{U}-\underline{B})$
2439000				2439000			
114.7214	1.831	-0.986	-1.451	114.7830	1.636	-0.926	-1.335
.7220	1.885	-0.977	-1.514	.7840	1.676	-0.943	-1.304
.7228	1.835	-0.925	-1.453	.7845	1.752	-1.043	-1.281
.7234	1.909	-1.030	-1.449	.7866	1.636	-0.967	-1.406
.7241	1.914	-1.007	-1.564	.7872	1.699	-1.029	-1.354
.7247	1.945	-1.049	-1.506	.7879	1.624	-0.833	-1.273
.7258	1.951	-1.038	-1.513	.7885	1.793	-1.016	-1.281
.7264	1.908	-1.042	-1.508	.7894	1.739	-0.952	-1.317
.7340	1.827	-0.969	-1.531	.7900	1.739	-0.991	-1.296
.7346	1.820	-0.940	-1.547	.7907	1.816	-0.918	-1.342
.7354	1.826	-0.929	-1.520	.7913	1.821	-0.936	-1.291
.7360	1.836	-0.978	-1.520	.7921	1.791	-1.028	-1.245
.7368	1.820	-0.958	-1.498	.7926	1.923	-1.027	-1.357
.7374	1.814	-0.929	-1.572	.7947	1.815	-0.813	-1.377
.7394	1.742	-0.923	-1.488	.7953	1.852	-0.937	-1.281
.7400	1.631	-0.852	-1.482	.7962	1.840	-1.071	-1.292
.7407	1.696	-0.921	-1.433	.7967	1.805	-0.965	-1.386
.7413	1.725	-0.927	-1.464	.7976	1.836	-0.968	-1.389
.7602	1.775	-0.887	-1.425	.7982	1.809	-0.965	-1.330
.7608	1.794	-0.912	-1.373	.7992	1.833	-0.945	-1.237
.7625	1.749	-0.971	-1.489	114.7998	1.832	-0.962	-1.259
.7631	1.623	-0.985	-1.421	120.70959	1.762	-1.036	-1.460
.7638	1.647	-0.949	-1.431	.71017	1.658	-0.969	-1.417
.7644	1.722	-0.961	-1.507	.71218	1.731	-1.000	-1.450
.7670	1.768	-0.896	-1.385	.71275	1.825	-1.035	-1.477
.7676	1.781	-0.907	-1.377	.71345	1.790	-0.964	-1.409
.7696	1.806	-0.901	-1.448	.71403	1.825	-0.988	-1.394
.7702	1.847	-0.942	-1.359	.71476	1.822	-0.926	-1.496
.7712	1.813	-1.021	-1.400	.71534	1.841	-0.957	-1.417
.7718	1.818	-0.921	-1.540	.71606	1.844	-0.929	-1.497
.7730	1.719	-0.942	-1.411	.71664	1.851	-0.974	-1.414
.7736	1.821	-1.041	-1.402	.71738	1.771	-0.938	-1.491
.7763	1.744	-0.986	-1.404	.71796	1.677	-0.910	-1.422
.7769	1.760	-0.938	-1.502	.71980	1.705	-0.961	-1.404
.7824	1.779	-1.075	-1.355	.72038	1.712	-0.901	-1.486

TABLE 3—Continued

Heliocentric JD	$\Delta \underline{V}$	$\Delta (\underline{B}-\underline{V})$	$\Delta (\underline{U}-\underline{B})$	Heliocentric JD	$\Delta \underline{V}$	$\Delta (\underline{B}-\underline{V})$	$\Delta (\underline{U}-\underline{B})$
2439000				2439000			
120.72120	1.757	-0.938	-1.446	120.75494	1.715	-0.947	-1.420
.72178	1.751	-0.993	-1.417	.75581	1.801	-1.008	-1.436
.72241	1.794	-0.998	-1.363	.75639	1.759	-0.953	-1.445
.72299	1.828	-0.971	-1.442	.75712	1.792	-0.987	-1.408
.72400	1.857	-0.990	-1.443	.75770	1.791	-0.962	-1.497
.72458	1.824	-0.959	-1.426	.75839	1.761	-0.937	-1.415
.72532	1.883	-1.006	-1.432	.75897	1.830	-1.007	-1.424
.72590	1.844	-1.010	-1.423	.76105	1.817	-1.053	-1.416
.72744	1.818	-1.069	-1.465	.76163	1.696	-0.984	-1.391
.72802	1.712	-0.999	-1.396	.76564	1.819	-0.956	-1.497
.72935	1.729	-0.956	-1.402	.76622	1.829	-0.949	-1.454
.72993	1.712	-0.929	-1.436	.76756	1.869	-1.002	-1.466
.73061	1.773	-0.946	-1.408	.76814	1.839	-0.956	
.73099	1.851	-1.028	-1.414	.76954	1.780	-0.975	-1.478
.73137	1.831	-0.959	-1.462	.77012	1.708	-0.962	-1.422
.73176	1.832	-0.985	-1.407	.77155	1.702	-0.996	-1.472
.73375	1.893	-1.083	-1.458	.77213	1.690	-0.962	-1.538
.73433	1.759	-0.987	-1.387	.77290	1.701	-0.923	-1.465
.73513	1.713	-1.038	-1.436	.77348	1.768	-1.008	-1.429
.73571	1.674	-0.977	-1.485	.77417	1.748	-0.961	-1.429
.73645	1.700	-0.975	-1.430	.77475	1.789	-0.964	-1.495
.73703	1.770	-0.991	-1.440	.77545	1.829	-1.022	-1.414
.74464	1.744	-0.981	-1.479	.77603	1.814	-0.962	-1.490
.74522	1.666	-0.979	-1.393	.77665	1.844	-1.026	-1.444
.74684	1.847	-1.097	-1.007	.77723	1.796	-0.956	-1.486
.74742	1.809	-1.033	-1.072	.77785	1.760	-0.916	-1.455
.74840	1.804	-0.982	-1.439	.77843	1.805	-0.955	-1.478
.74898	1.778	-0.922	-1.418	.77904	1.787	-1.036	-1.426
.74965	1.786	-0.947	-1.439	.77962	1.577	-0.903	-1.400
.75023	1.834	-1.019	-1.429	.78903	1.712	-0.924	-1.507
.75100	1.774	-0.951	-1.428	.78961	1.735	-0.896	-1.502
.75157	1.709	-0.941	-1.389	.79106	1.827	-1.022	-1.446
.75309	1.678	-0.962	-1.422	.79164	1.878	-1.061	-1.404
.75357	1.708	-1.045	-1.424	.79352	1.815	-0.988	-1.421

TABLE 3—Continued

Heliocentric JD	$\Delta \underline{V}$	$\Delta (\underline{B}-\underline{V})$	Heliocentric JD	$\Delta \underline{V}$	$\Delta (\underline{B}-\underline{V})$	$\Delta (\underline{U}-\underline{B})$
2439000			2439000			
120.79486	1.763	-0.945	120.82591	1.765	-0.901	-1.489
.79544	1.732	-0.912	.82897	1.872	-0.996	-1.484
.79687	1.519	-0.942	.82955	1.875	-0.961	-1.490
.79745	1.669	-1.024	.83015	1.844	-0.916	-1.502
.79809	1.694	-0.935	.83073	1.892	-1.037	-1.453
.79867	1.788	-0.950	.83138	1.830	-1.052	-1.570
.79929	1.781	-0.950	.83196	1.654	-1.017	-1.475
.79987	1.853	-0.987	.83260	1.637	-1.027	-1.465
.80043	1.887	-0.956	.83318	1.710	-1.059	-1.495
.80101	1.863	-0.985	.83381	1.763	-1.017	-1.391
.80159	1.827	-0.934	.83439	1.846	-1.064	-1.441
.80216	1.811	-0.941	.83498	1.857	-1.035	-1.443
.80361	1.792	-1.023	.83556	1.884	-1.029	-1.430
.80419	1.636	-1.002	.83711	1.895	-1.061	-1.455
.80481	1.591	-0.947	.83768	1.891	-1.055	-1.445
.80539	1.759	-1.043	.83831	1.912	-1.115	-1.405
.80612	1.739	-0.960	.83889	1.900	-1.082	-1.475
.80670	1.745	-0.967	.83972	1.820	-1.132	-1.492
.80735	1.708	-0.929	.84030	1.682	-1.021	-1.435
.80793	1.775	-0.981	.84094	1.671	-1.040	-1.422
.80889	1.806	-0.958	.84152	1.639	-0.975	-1.511
.80947	1.807	-0.990	.84240	1.775	-1.073	-1.367
.81088	1.826	-1.026	.84297	1.838	-1.064	-1.446
.81146	1.844	-0.980	.84440	1.814	-0.976	-1.472
.81219	1.807	-1.040	.84498	1.865	-1.032	-1.485
.81277	1.630	-0.880	.84566	1.885	-1.059	-1.366
.81338	1.708	-0.997	.84624	1.821	-0.998	-1.487
.81396	1.722	-1.038	.84686	1.812	-1.007	-1.465
.81466	1.811	-1.034	.84744	1.765	-0.985	-1.420
.81524	1.703	-0.951	.84891	1.507	-1.025	-1.475
.81590	1.706	-0.925	.84949	1.633	-1.080	-1.510
.81648	1.790	-0.959	.85016	1.641	-0.990	-1.455
.81707	1.744	-0.895	.85074	1.775	-1.079	-1.489
.81765	1.787	-0.928	.85229	1.754	-1.024	-1.458
.81823	1.777	-0.928	.85287	1.760	-0.981	-1.451

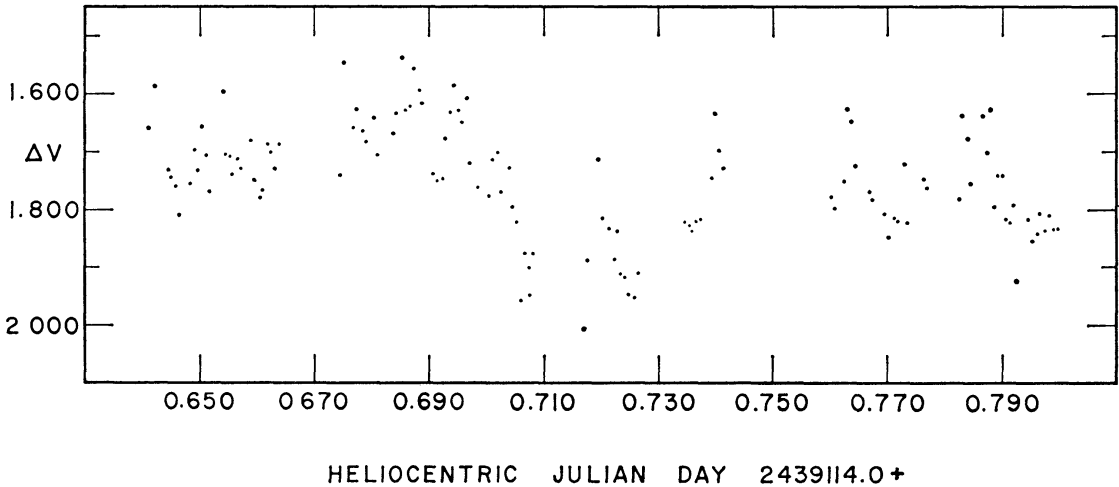


FIG. 3.—Plot of differential V -magnitude brightness variation versus heliocentric Julian day for the blue variable for December 20, 1965, U.T. The differential magnitude is in the sense variable *minus* comparison star.

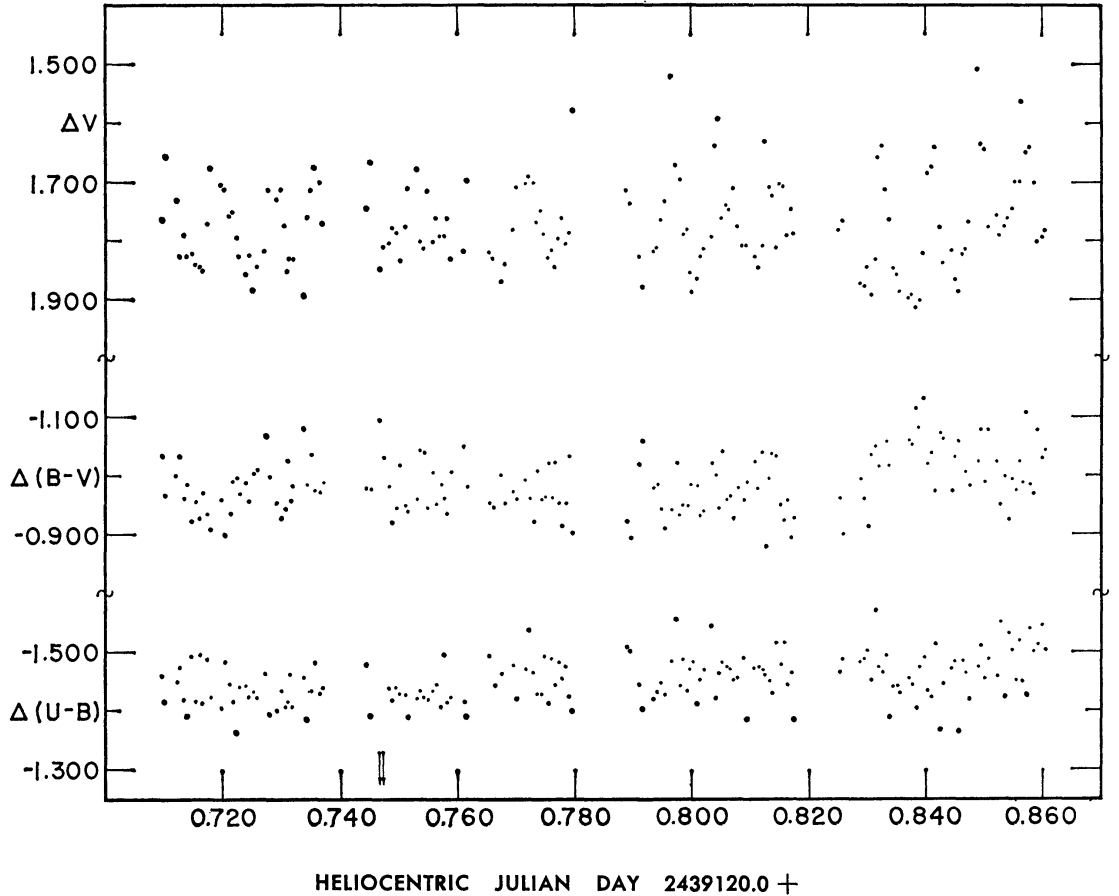


FIG. 4.—Plot of differential UBV magnitudes and colors versus heliocentric Julian day for the blue variable for December 26, 1965, U.T. The differential quantities are in the sense variable *minus* comparison star.

min was scanned. Note that the average background noise level is just under 0.030 mag. The task of identifying the proper period, as evidenced by a frequency peak, can be relatively straightforward if one peak stands out above all others. However, the results displayed in Figure 6 do not in themselves permit a clear-cut decision. Recourse to Figures 2-5 hints at a period on the order of 12^m5 . Therefore, the highest peak in Figure 6 at a frequency of $726.3 \text{ rad day}^{-1}$ was chosen as the peak in the computed spectrum which most closely corresponded to an indicated period of 12^m5 in the variable-star raw data.

The removal of the peak at $726.3 \text{ rad day}^{-1}$ resulted not only in a spectrum (not illustrated) whose average noise level fell below 0.020 mag, but also in the removal of smaller spurious peaks at 1750, 1304, 1135, 1040, 880, 584, and 450 rad day^{-1} . Somewhat successful efforts were made to remove additional peaks, including some of those which appeared after the initial prewhitening with respect to the 12^m457 period ($726.3 \text{ rad day}^{-1}$). Usually

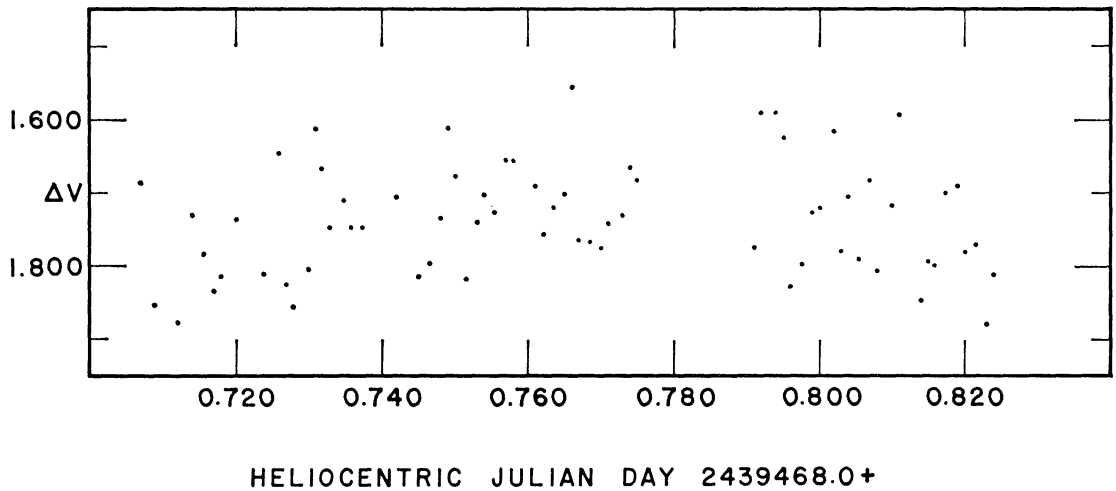


FIG. 5.—Plot of differential *V* magnitude versus heliocentric Julian day for the blue variable for December 9, 1966, U.T. The differential magnitude is in the sense variable *minus* comparison star.

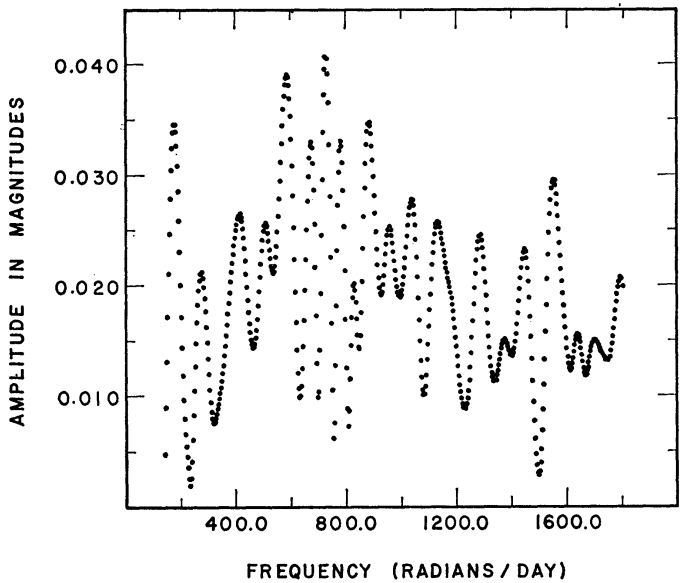


FIG. 6.—Portion of spectrum computed for data of December 26, 1965, U.T. based on the techniques of Wehlau and Leung (1964).

when given peak(s) were removed, others popped up elsewhere, which leads one to doubt the physical reality of the peaks being subtracted from the spectrum. Furthermore, the background noise level of 0.018 mag remained substantially constant. It is of interest to note both now and for what follows that the lowest noise level that was calculated corresponded roughly to the accuracy of the differential photometric data.

Since the blue variable was thought to be a white dwarf (Haro and Luyten 1961) and since evidence exists for very short-period variations in white-dwarf-like objects (Walker 1961), the ΔV -magnitude data for December 26, 1965, U.T. was also scanned at higher frequencies in search of a period between 1^m9 and 5^m6 . The resulting spectrum, not illustrated here, showed a rather uniform noise level of 0.024 mag with no really predominant

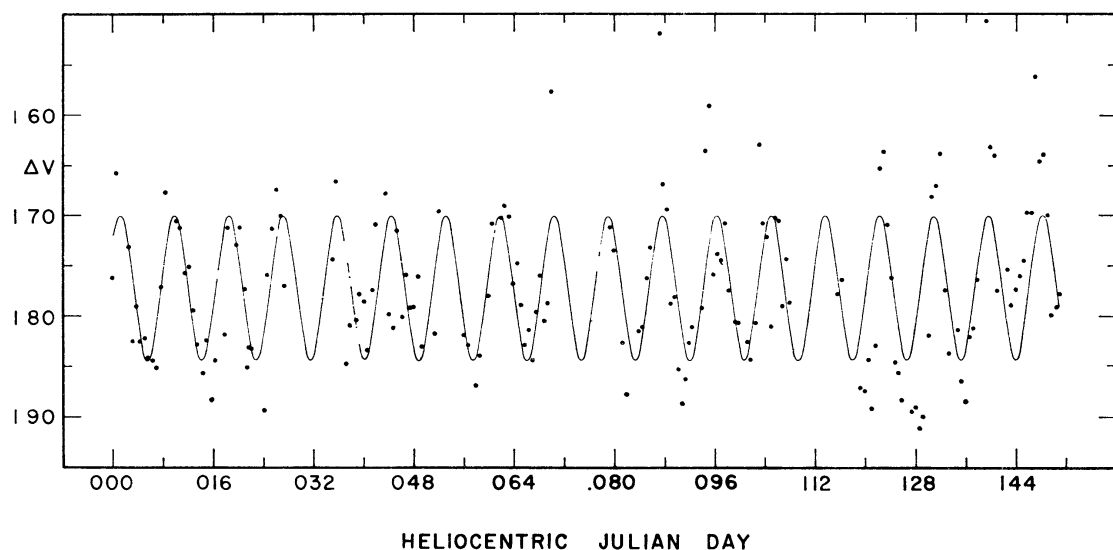


FIG. 7.—Sine curve of amplitude 0.14 mag and period $12^m45.7$ superimposed upon the raw data of Fig. 4 for December 26, 1965, U.T.

peaks. The high-frequency spectrum was then prewhitened with respect to the $12^m45.7$ period found above. The result was a lowering of the over-all noise level to 0.016 mag, again without the appearance of additional peaks. The periodogram analysis, then, indicates that on December 26, 1965, U.T. the blue variable varied by 0.14 mag with a period of $12^m45.7$. Figure 4 shows the maximum observed amplitude of variation to be approximately 0.25 mag. A sine curve of amplitude 0.14 mag and frequency $726.3 \text{ rad day}^{-1}$ was then superimposed on the raw data illustrated in Figure 4 via a computer program (Hill 1967). The resulting plot via the Louisiana State University's Research Computer Center Calcomp plotter is displayed in Figure 7. The agreement is reasonable.

It is evident in Figure 7, however, that the scatter in the latter half of the December 26, 1965, U.T. observing run is greater than during the first half of the night. Therefore, the data were analyzed in two sections, with the division being taken at heliocentric Julian day 2439120.785, a natural break in the data caused by observations of the comparison stars and *UBV* standards. The analysis of the data from the first half of the night gave a period of $12^m48.8$ and an amplitude of light variation of 0.12 mag, whereas the second half of the data gave a period of $12^m57.7$ and an amplitude of 0.17 mag.

A similar analysis of the raw data for December 9, 1966, U.T., illustrated in Figure 5, resulted in the spectrum shown in Figure 8. In this instance, a single strong peak is present at a frequency of $724.3 \text{ rad day}^{-1}$ which corresponds to a period of $12^m49.1$. The background noise level of the spectrum of approximately 0.016 mag is similar to that

found for the data discussed above for December 26, 1965, U.T. Figure 9 illustrates the spectrum resulting upon subtraction of the peak at $724.3 \text{ rad day}^{-1}$ with its corresponding amplitude from the spectrum shown in Figure 8. In this instance the background noise level increased slightly.

The light curve for December 20, 1965, U.T., illustrated in Figure 3, indicates that the object varied 0.4 mag that night; analysis of the V data gives an approximate $14^{\text{m}}1$ period of variation. This night's periodogram (not illustrated) possesses only a few very broad peaks and is quite unlike the periodograms previously discussed, as Figure 3 might cause one to suspect.

In summary, then, analysis of the photoelectric data indicates the presence of a $12^{\text{m}}5$ light variation. Since a study of the differential color curves showed essentially no secular change in the color of the object, the magnitude of the light variation is equivalent at all three effective wavelengths, i.e., U , B , V . One can speculate that the object is probably a single star pulsating with a basic period of $12^{\text{m}}5$ with other beat periods still to be determined. However, after considerable time spent in trying to remove peaks from periodograms only to see them pop up elsewhere, it seemed prudent to push the period analysis no further at this moment. A further possibility which arises from contemplation

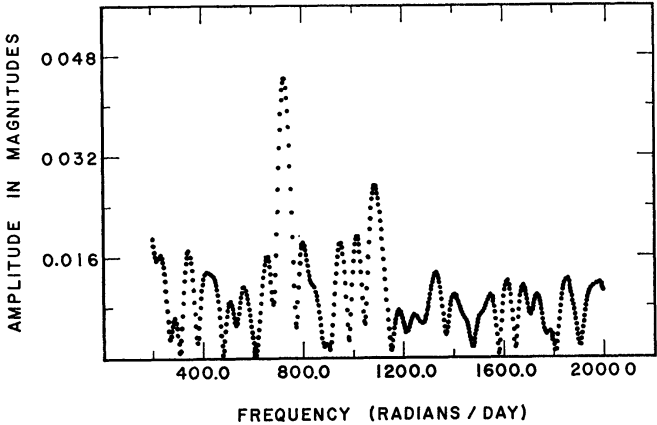


FIG. 8.—Portion of spectrum computed for the data of December 9, 1966, U.T.

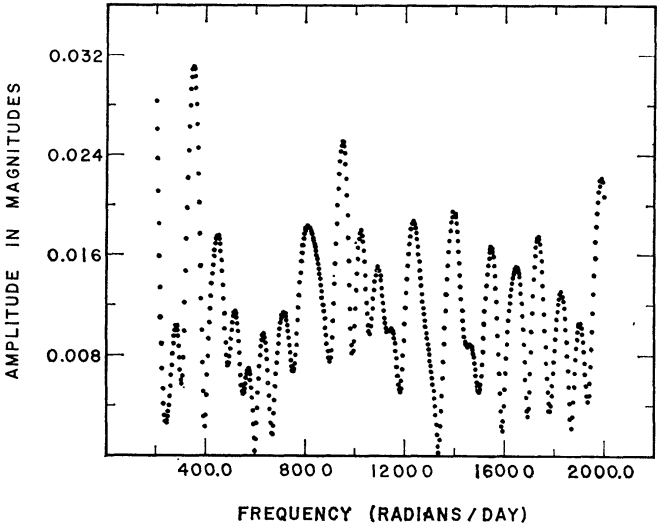


FIG. 9.—Spectrum illustrated in Fig. 8 prewhitened with respect to a frequency of $724.3 \text{ rad day}^{-1}$

of Figure 3 is that an eclipse might have occurred near heliocentric Julian day 2439114.715; then the short-period variations would have to be ascribed to one component of the eclipsing system. Similar-appearing effects and light curves have been found for U Gem stars and old novae (Mumford 1967).

The work of Haro and Luyten (1961) indicates a proper motion of $0''.1$ per year in 143° . The average magnitude and colors for the blue variable as calculated from all observations are $V = 14.965$, $(B - V) = +0.205$, and $(U - B) = -0.500$ mag. Through use of an empirical statistical relation between apparent magnitude, absolute magnitude, and proper motion (Greenstein 1958), one can determine $M_V = +10.7$ mag. The distance to the dark cloud in Taurus against which the blue variable is projected is 125 pc (McCuskey 1939). This provides an upper limit to the blue variable's distance and hence a lower limit to its parallax, i.e., $0''.008$. Hence, from $M_V = m_V + 5 + 5 \log p$, one has $M_V = +9.5$ mag as an upper limit to its luminosity. It is also possible to show that the tangential velocity of the object is about 34 km sec^{-1} , which, from Greenstein's (1958) discussion, is a reasonable value. Relations between M_V and the $(U - V)$ color index for white dwarfs have been presented by Eggen and Greenstein (1965). Their Figure 4 indicates the division of white dwarfs in the M_V , $U - V$ plane into two groups: members in the first group satisfy the relation $M_V = +11.65 + 0.85(U - V)$, and those in the second group show a larger scatter about a similar but steeper relation whose zero point is 1.5 mag fainter. Given $(U - V) = -0.295$ mag for the blue variable under discussion, one therefore finds its M_V to be $+11.4$ mag or approximately 13.0 mag, depending on whether the object belongs to the first group or to the second. A summary of the absolute-magnitude considerations in this paragraph permits the statement that the blue variable is most probably a white dwarf.

Image-tube spectrograms have been obtained through continuous trailing of the plateholder at a uniform rate along the slit without repetition at the Cassegrain focus of the KPNO 84-inch reflector. A variety of dispersions from 242 to 47 \AA mm^{-1} have been used. The spectrograms were obtained on Kodak IIaO spectroscopic plates with the aid of an English Electric Valve P829D image intensifier. Those spectrograms obtained at 47 \AA mm^{-1} , an example of which is shown in Figure 10 (Plate 5), show the K-line of Ca II in addition to the hydrogen lines. The latter are $35\text{--}40 \text{ \AA}$ in width and provide further evidence that the object is indeed a white dwarf. The highest Balmer line visible on any spectrogram was $H\theta$. Eggen and Greenstein's (1965) Figure 6 permits a temperature estimate of 9650°K to be made. No emission features are definitely identifiable. The blue variable may be a new addition to a group of six white dwarfs classified as type DA, F, or DF by Eggen and Greenstein (1965) in their Table 1. The spectral features of this type of white dwarf show both hydrogen lines and a weak K-line (Greenstein 1958; Eggen and Greenstein 1965), just the features possessed by the blue variable. The average UBV colors of the six DF-type white dwarfs are $(B - V) = +0.29$ and $(U - B) = -0.60$ mag; inclusion of the blue variable in the group changes the average color index for the group by less than 2 per cent.

Short-period fluctuations have been known to occur in the apparent brightnesses of hot subluminal variable stars (Herbig 1965; Williams 1966), in novae and nova-like variables as summarized by Mumford (1967), in the peculiar white dwarf HZ 29 (Smak 1967) and in X-ray sources (Hiltner and Mook 1967; Mook 1967; Kristian, Sandage, and Westphal 1967). In the case of DQ Her, an old nova composed of a white dwarf and a faint red companion, light fluctuations whose periodicity is that of the fundamental period of pulsation of the white dwarf have been detected (Walker 1961). The present blue variable so far has been considered to be a single pulsating star with a beat period primarily because attempts in phasing the data have been unsuccessful, i.e., it has not been possible to compile a composite light curve such as Smak (1967) has constructed for HZ 29. On the other hand, the blue variable may be an eclipsing system, since it appears from differential measurements of the hydrogen lines on the 47 \AA mm^{-1} spectrograms

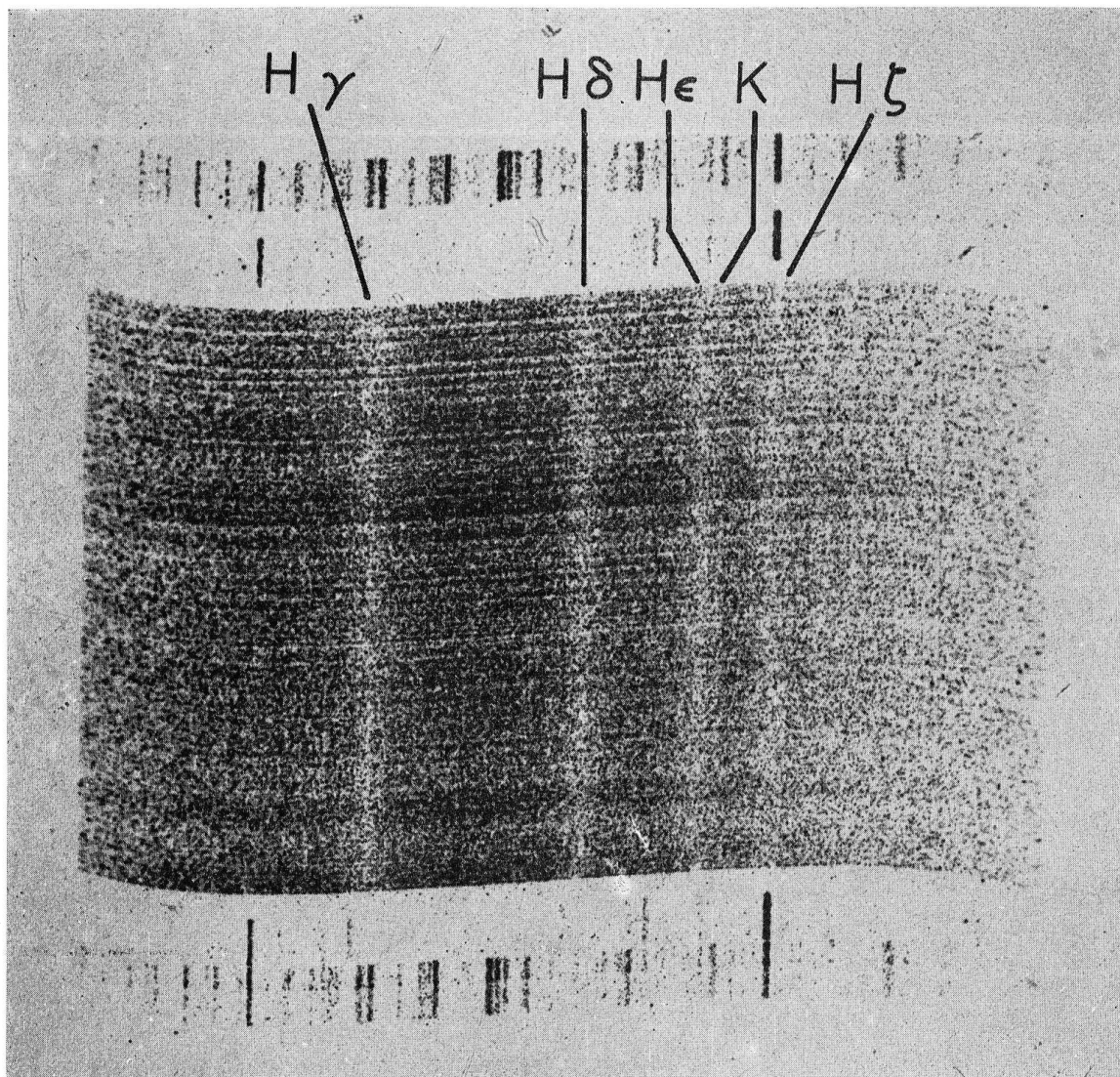


FIG. 10.—Image-tube spectrum of the blue variable showing the hydrogen lines $H\gamma$, $H\delta$, $H\epsilon$, and $H\zeta$ together with the K-line of Ca II at a dispersion of 47 \AA mm^{-1} . The comparison source used was $\text{He} + \text{Ar} + \text{Ne}$.

LANDOLT (*see* page 163)

that the radial velocity varies with an amplitude of perhaps 500 km sec^{-1} . At the same time, the radial velocity of the K-line of Ca II on these same spectra appears to be constant. Perhaps one could then explain the inability to construct a composite light curve by hypothesizing the intrinsic variability of either or both of the components. However, the continuous trailing of the plateholder technique has so far failed to provide spectrograms which show the S-shaped curve (Kraft, Mathews, and Greenstein 1962) which would announce the presence of a binary system. If the object is composed of two equally luminous white dwarfs, then the period would be 25 min. Since the radial velocity of the K-line appears constant, its intensity is most probably due to interstellar absorption in the direction of the Taurus cloud. If only one component of the hypothesized binary system were a white dwarf, then the second component would have to be not only a red dwarf less luminous than $M_V = +12.0 \text{ mag}$ but also faint enough so that its spectrum was not visible.

The encouragement of Drs. A. Sandage and H. Abt and the assistance and hospitality of the Kitt Peak National Observatory staff are gratefully acknowledged. In particular, thanks are due Dr. R. Lynds for his unstinting efforts at the telescope with his image-tube spectrograph in obtaining the spectrograms and Mr. R. Barnes and Mr. J. C. Golson for assistance during the photometric observing runs. The comments of Dr. G. Hill and the assistance of both Dr. Hill and Mr. L. M. Cook at the Louisiana State University computer, supported in part by NSF funds, is also acknowledged. This variable-star study was supported by the National Science Foundation.

REFERENCES

- Eggen, O. J., and Greenstein, J. L. 1965, *A p. J.*, **141**, 83.
 Greenstein, J. L. 1958, *Hdb. d. A p.* (Berlin: Springer-Verlag), **50**, 166.
 Haro, G., and Luyten, W. J. 1961, *Bol. Obs. Tonantzintla y Tacubaya*, **3**, 35, No. 21.
 Herbig, G. H. 1965, *Trans. I.A.U.*, **12A**, 385.
 Hill, G. 1967 (private communication).
 Hiltner, W. A., and Mook, D. E. 1967, *A p. J. (Letters)*, **150**, L23.
 Kelsall, T. 1966 (private communication).
 Kraft, R. P., Mathews, J., and Greenstein, J. L. 1962, *A p. J.*, **136**, 312.
 Kristian, J., Sandage, A., and Westphal, J. A. 1967, *A p. J. (Letters)*, **150**, L99.
 Landolt, A. U. 1967, *A. J.*, **72**, 1012.
 McCuskey, S. W. 1939, *A p. J.*, **89**, 583.
 Mook, D. E. 1967, *A p. J. (Letters)*, **150**, L25.
 Mumford, G. S. 1967, *Pub. A.S.P.*, **79**, 283.
 Smak, J. 1967, *Acta Astr.*, **17**, 255.
 Walker, M. F. 1961, *A p. J.*, **134**, 171.
 Wehlau, W., and Leung, K.-C. 1964, *A p. J.*, **139**, 843.
 Williams, J. D. 1966, *Pub. A.S.P.*, **78**, 279.

Copyright 1968. The University of Chicago. Printed in U S A.